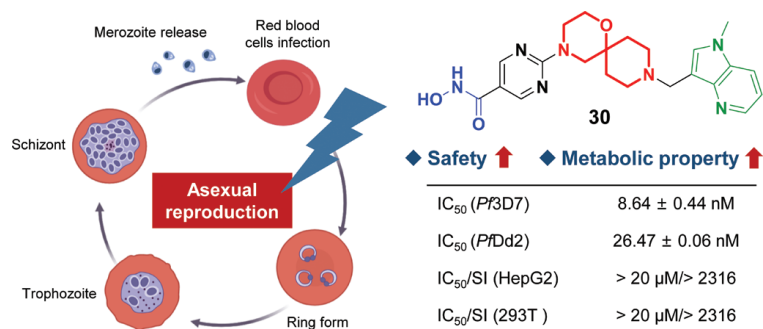


# Design and synthesis of novel hydroxamic acid derivatives based on quisinostat as promising antimalarial agents with improved safety

## Graphical abstract



## Authors

Manjiong Wang, Tongke Tang,  
Zhenghui Huang, Ruoxi Li,  
Dazheng Ling, Jin Zhu,  
Lubin Jiang, Jian Li, Xiaokang Li

## Correspondence

xkli@ecust.edu.cn (X. Li);  
jianli@ecust.edu.cn (J. Li);  
lbjiang@ips.ac.cn (L. Jiang)

## Highlights

- Compound **30** exhibited significant antimalarial activity against both wild-type and multidrug-resistant malarial parasites.
- Compound **30** displayed completely elimination of parasites in the murine *P. yoelii* model.
- Compound **30** considerably reduced cytotoxicity and ameliorated metabolic properties compared with lead compound quisinostat.
- Compound **30** was confirmed to kill *P. falciparum* parasites by inhibiting PfHDAC enzymes activity.

## In brief

In this work, 38 novel hydroxamic acid derivatives were designed and synthesized based on clinical phase II antitumor HDAC inhibitor quisinostat. Among them, the optimal compound **30** retained significant antimalarial activity both *in vitro* and *in vivo*, while improving safety and metabolic properties.

## Research Article

# Design and synthesis of novel hydroxamic acid derivatives based on quisinostat as promising antimalarial agents with improved safety

Manjiong Wang<sup>a,1</sup>, Tongke Tang<sup>b,f,1</sup>, Zhenghui Huang<sup>b</sup>, Ruoxi Li<sup>a</sup>, Dazheng Ling<sup>a</sup>, Jin Zhu<sup>a</sup>, Lubin Jiang<sup>b,f,\*</sup>, Jian Li<sup>a,c,d,e,\*</sup>, Xiaokang Li<sup>a,\*</sup>

<sup>a</sup>State Key Laboratory of Bioreactor Engineering, Shanghai Frontiers Science Center of Optogenetic Techniques for Cell Metabolism, Frontiers Science Center for Materiobiology and Dynamic Chemistry, Shanghai Key Laboratory of New Drug Design, School of Pharmacy, East China University of Science and Technology, Shanghai 200237, China

<sup>b</sup>Key Laboratory of Molecular Virology and Immunology, Institut Pasteur of Shanghai, University of Chinese Academy of Sciences, Chinese Academy of Sciences, Shanghai 200031, China

<sup>c</sup>Yunnan Key Laboratory of Screening and Research on Anti-pathogenic Plant Resources from West Yunnan, College of Pharmacy, Dali University, Dali 671000, China

<sup>d</sup>Clinical Medicine Scientific and Technical Innovation Center, Shanghai Tenth People's Hospital, Tongji University School of Medicine, Shanghai 200092, China

<sup>e</sup>Key Laboratory of Tropical Biological Resources of Ministry of Education, College of Pharmacy, Hainan University, Haikou 570228, Hainan, China

<sup>f</sup>School of Life Science and Technology, ShanghaiTech University, Shanghai 201210, P.R. China

<sup>1</sup>These authors contributed equally to this work: Manjiong Wang, Tongke Tang.

\*Correspondence: xkli@ecust.edu.cn (X. Li); jianli@ecust.edu.cn (J. Li); lbjiang@ips.ac.cn (L. Jiang)

Received: 17 March 2022; Revised: 02 May 2022; Accepted: 03 May 2022

Published online: 17 May 2022

DOI: 10.15212/AMM-2022-0007

## ABSTRACT

In our previous work, the clinical phase II HDAC inhibitor quisinostat was identified as a promising antimalarial agent through a drug repurposing strategy, but its safety was a matter of concern. Herein, further medicinal chemistry methods were used to identify new chemical entities with greater effectiveness and safety than quisinostat. In total, 38 novel hydroxamic acid derivatives were designed and synthesized, and their *in vitro* antimalarial activities were systematically investigated. These compounds at nanomolar concentrations showed inhibitory effects on wild-type and drug-resistant *Plasmodium falciparum* strains in the erythrocyte stage. Among them, compound **30**, after oral administration, resulted in complete elimination of parasites in mice infected with *Plasmodium yoelii*, and also exhibited better safety and metabolic properties than observed in our previous work. Mechanistically, compound **30** upregulated plasmodium histone acetylation, according to western blotting, thus suggesting that it exerts antimalarial effects through inhibition of *Plasmodium falciparum* HDAC enzymes.

**Keywords:** antimalarial, drug repurposing, hydroxamic acid, erythrocyte stage, drug resistance

## 1. INTRODUCTION

Malaria is one of the oldest and deadliest infectious diseases and has been a public-health challenge worldwide. According to the World Malaria Report 2021, an estimated 241 million cases of malaria and 627,000 deaths due to malaria occurred in 2020, representing an increase of 14 million malaria cases and 69,000 deaths over 2019 [1]. The rise in malaria cases and deaths has been partly associated with the disruption of malaria services due to the COVID-19 outbreak in 2019 [2, 3];

however, global progress against malaria had already stalled before the outbreak. Although the World Health Organization has recommended widespread use of the RTS,S/AS01 vaccine to prevent malaria in young children in Africa, the vaccine does not provide 100% protection [4]. Therefore, chemotherapy drugs are important treatments. However, the emergence and spread of drug-resistant malaria has been the largest public health emergency in malaria control. Alarmingly frequent emergence of artemisinin-resistant strains has been observed in Southeast Asia and Africa in

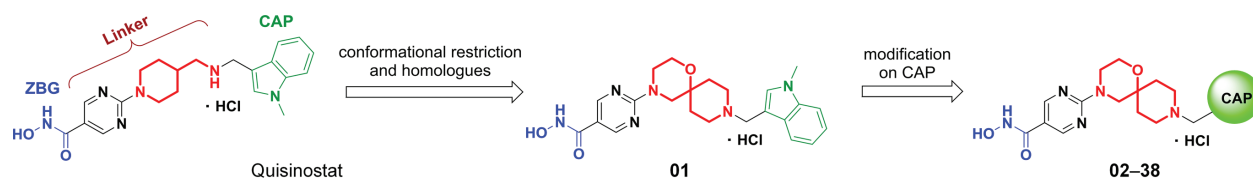


Figure 1 | Design of novel hydroxamic acid derivatives.

recent years [5-9], thus posing a challenge to the use of artemisinin-based combination therapies as first-line treatments [10]. Therefore, the development of new antimalarial drugs effective against resistant plasmodium is a major scientific and public health need that must urgently be addressed.

To solve the problem of drug resistance, medicinal chemists have aimed to develop new chemical agents with different targets and mechanisms of action from those of existing antimalarial drugs [11-15]. Studies are increasingly revealing that histone deacetylase (HDAC) inhibitors have potent killing effects against plasmodium *in vitro* and *in vivo* [16-21]. HDACs play important roles in eukaryotic cellular chromatin structure, transcription and gene expression [22]. To date, five *Plasmodium falciparum* HDACs (*Pf*HDACs) have been identified; these enzymes influence plasmodium survival by modulating gene expression, virulence, antigenic variation and cytoadhesion [23-25].

In our previous studies, the clinical phase II anti-cancer HDAC inhibitor quisinostat was identified as a promising antimalarial agent; however, this compound has high toxicity. The structural modification of quisinostat has been demonstrated to decrease its toxicity while retaining potent antimalarial activity; further experiments have confirmed that its derivatives have *Pf*HDAC inhibitory activity [26-28]. The work herein was aimed at exploring a new structural framework to further improve the drug's safety and broaden the therapeutic window. Referring to successful previous studies, we retained the hydroxamic acid fragment as the zinc-binding group and replaced the 4-aminomethylpiperidine moiety of the linker with a 1-oxa-4,9-diazaspiro[5.5]undecane moiety to increase the rigidity of the compounds through conformational restriction. The *N*-methylindole fragment (CAP region) was then systematically modified to fully explore the structure-activity relationships (SARs) and further improve bioactivity (Figure 1). Finally, a total of 38 derivatives with new structural frameworks were obtained.

## 2. METHODS

### 2.1. Compound synthesis

The synthetic methods for compounds 01-38 are depicted in Scheme 1. Compound A was obtained through a nucleophilic aromatic substitution reaction between ethyl 2-chloropyrimidine-5-carboxylate and

*tert*-butyl 1-oxa-4,9-diazaspiro[5.5]undecane-9-carboxylate under alkaline conditions; the *tert*-butoxycarbonyl (Boc) group was then removed in a solution of hydrochloric acid/dioxane to obtain compound B. Compound B underwent reductive amination, thus yielding intermediates C01-C38. Next, the ethyl ester of C01-C38 was hydrolyzed and condensed with *O*-(tetrahydro-2*H*-pyran-2-yl)hydroxylamine (THPONH<sub>2</sub>) to acquire intermediates D01-D38. Finally, target compounds 01-38 were obtained through deprotection in a solution of hydrochloric acid/dioxane. The detailed synthesis and characterization of the final compounds 01-38 are documented in the Supporting Information.

### 2.2. Parasite culture

The parasite strains used in this work were all cultured in RPMI 1640 medium (Gibco) supplemented with sodium bicarbonate (2.2 g/L), Albumax (5 g/L), HEPES (5.94 g/L), hypoxanthine (50 mg/L) and gentamycin (50 mg/L) in an atmosphere consisting of 5% O<sub>2</sub>, 5% CO<sub>2</sub> and 90% N<sub>2</sub> [29].

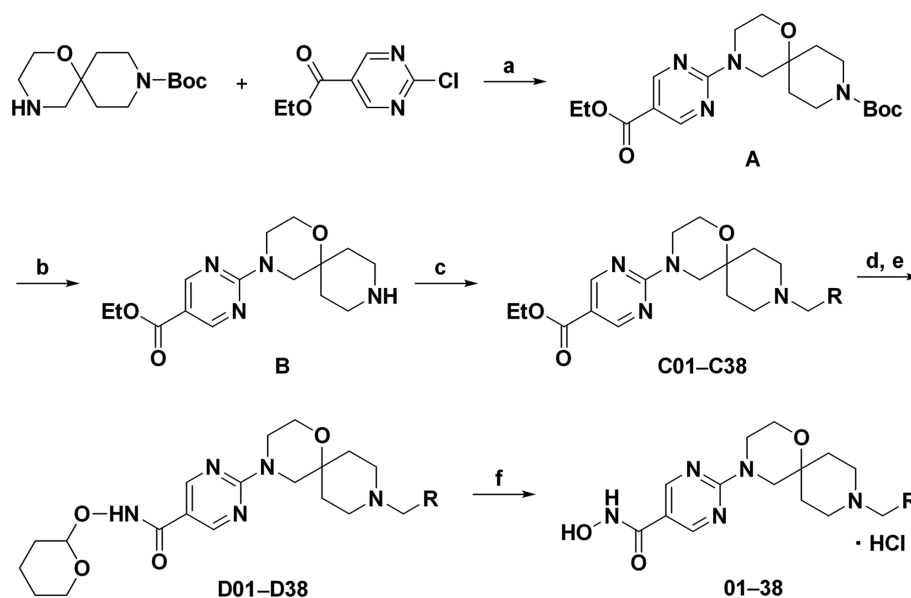
### 2.3. *In vitro* 72 h erythrocyte-stage parasite-killing assays

Highly synchronized ring-stage parasites (1% parasitemia and 2% hematocrit) were cultured in 96-well plates with a total volume of 200  $\mu$ L of compound. The compounds were serially diluted from an initial concentration of 200 nM. After 72 hours of incubation, 100  $\mu$ L of dissolution buffer (0.12 mg/mL saponin, 0.12% Triton X-100, 30 mM Tris-Cl and 7.5 mM EDTA) was added to dissolve the parasites. Each well was then stained with SYBR Green I (Invitrogen; supplied at 10,000 $\times$  dilution) and incubated in the dark for 2 hours [30]. Under 485 nm excitation and 535 nm emission conditions, the fluorescence signal representing parasite DNA was monitored with a microplate reader (Bioteck, Synergy H1). The IC<sub>50</sub> was calculated in GraphPad 7. The results are shown as the mean  $\pm$  SD from two independent experiments.

### 2.4. *In vitro* cytotoxicity assays

HepG2 and 293T cells were cultured in DMEM (HyClone) supplemented with 10% FBS (Gibco) and 1% penicillin/streptomycin (YEASEN) at 37°C under 5% CO<sub>2</sub>. Cells (70,000 cells/mL) were seeded in 96-well plates in a total volume of 100  $\mu$ L and were cultured for 24 h. Tested compounds were added to the plate (two-fold dilutions ranging from 20  $\mu$ M to 0.049  $\mu$ M), and cell

## Research Article



**Scheme 1 | Synthesis of compounds 01-38.**

Reagents and conditions: (a) DIPEA, DCM, 0°C to room temperature, 2–3 h; (b) HCl in 1,4-dioxane, DCM, room temperature, 5–6 h; (c) RCHO, NaBH(OAc)<sub>3</sub>, HOAc, DCE, room temperature, overnight; (d) K<sub>2</sub>CO<sub>3</sub>, MeOH:H<sub>2</sub>O = (1:1), 65–70°C, 8–12 h; (e) THPONH<sub>2</sub>, EDCl, HOBT, Et<sub>3</sub>N, DMF, room temperature, 48 h; (f) HCl in 1,4-dioxane, DCM, room temperature, 30 min.

culture continued for 72 h. Then 10% Cell Counting Kit 8 (YEASEN) reagent was added to each well for the analysis of cell viability. The absorbance was monitored after 2 h at 450 nm with a microplate reader (Biotech, Synergy H1). The IC<sub>50</sub> was calculated in GraphPad 7. The results are shown as the mean ± SD from two independent experiments.

## 2.5. Mouse liver microsome metabolism assays

This experiment was performed by Shanghai ChemPartner Co., Ltd. Liver microsomes (0.5 mg/mL) were purchased from Corning Corporation. Ketanserin was used as a positive control. First, the tested compounds were dissolved in DMSO (10 mM) and then diluted to 0.5 mM with acetonitrile. The compounds were then adjusted to a working concentration of 1.5 μM in liver microsomal buffer; 30 μL was mixed with 15 μL of 6 mM NADPH at 37°C. At 0, 5, 15, 30 and 45 minutes after incubation, 135 μL of acetonitrile was added to stop the reaction. The mixture was incubated on a shaker (IKA, MTS 2/4) at 600 rpm/min for 10 min, then centrifuged at 5594×g for 15 min (Thermo Multifuge×3R). The supernatant was diluted 1:1 with distilled water and analyzed by LC-MS/MS.

## 2.6. In vivo erythrocytic antimalarial assays

All animal experimental procedures followed the National Institutes of Health Guide for the Care and Use of Laboratory Animals under the supervision of the Animal Welfare Committee of Institute Pasteur of Shanghai, Chinese Academy of Sciences (IACUC issue No.

A2018009). Each group contained five female BALB/c mice (6–8 weeks of age). At day 0, each mouse was i.p. inoculated with 10<sup>5</sup> *P. yoelii* parasites [31]. After 24 h, the solution of compounds (DMSO: 20 wt% aqueous 2-hydroxypropyl-β-cyclodextrin = 5:95 v/v) or solvent was delivered p.o. at the indicated dose once daily for five successive days. Piperaquine phosphate (PPQ) was used as a positive control and was delivered i.p. Parasitemia was counted from at least 5,000 red blood cells by smearing at days 6, 30 and 60. The graph was generated in GraphPad 7.

## 2.7. Western blot assays

First, the red blood cells in parasite samples were removed with 0.15% saponin, and the parasites were sonicated in 1% NP-40 lysis buffer. After centrifugation at 12,000×g for 15 min, the supernatant was resuspended in regular SDS loading buffer. Parasite proteins were separated with 10% SDS-PAGE and transferred to a PVDF membrane (Millipore). Antibodies to acetylated histone H3 (H3; Millipore; 06-599) or H3 (ABclonal; A2348) were used for immunodetection; the secondary antibody was conjugated to HRP (Jackson ImmunoResearch). Signal detection was performed with a chemiluminescent HRP substrate Immobilon-Western kit (Millipore).

## 2.8. Human HDAC inhibition assays

This experiment was performed by Shanghai ChemPartner Co., Ltd. Human HDACs 1–3, 6 and 8, and SIRT 2 were purchased from BPS. SAHA and suramin were used as positive controls. The tested compounds

were threefold diluted from the initial concentration of 10  $\mu$ M and then were incubated with 15  $\mu$ L enzyme/Tris buffer at room temperature for 15 min. Subsequently, 10  $\mu$ L trypsin and Ac-peptide substrate/Tris buffer were added to start the reaction, and HDACs 1–3, 6 were incubated at room temperature. To start the reaction, 10  $\mu$ L Ac-peptide substrate/Tris buffer was added and incubated at room temperature for 4 h. Subsequently, HDAC 8 and SIRT 2 were incubated with trypsin solution for 2 h. Enzymatic activity was measured with a Synergy MX instrument with excitation at 355 nm and emission at 460 nm. The  $IC_{50}$  was calculated in GraphPad 7.

### 2.9. Pharmacokinetic assays

This experiment was performed by Shanghai ChemPartner Co., Ltd. Female BALB/c mice (6–8 weeks of age) were bred and acclimated for 1 week. The compounds were dissolved in 5% DMSO and diluted to 0.5 mg/ml with 20% aqueous 2-hydroxypropyl- $\beta$ -cyclodextrin solution (stock concentration). Each mouse was intraperitoneally injected with a compound solution at a dose of 5 mg/kg. Blood samples were collected into tubes containing anticoagulant ( $K_2$ -EDTA) at 0.25, 0.5, 1, 2, 4, 8 and 24 h after injection and centrifuged at 2,000 $\times$ g at 4°C for 5 min to obtain plasma. LC-MS/MS of samples was performed on an ACQUITY UPLC HSS T3 1.8  $\mu$ m column. The mobile phase was a mixture of phase A (0.1% formic acid in water) and phase B (0.1% formic acid in acetonitrile), and gradient mode was used with a flow rate of 0.6 mL/min at 60°C. Mass spectra were acquired on an API6500 triple quadrupole instrument equipped with an ESI source. Propranolol was used as the internal standard. Plasma concentrations of compounds were analyzed, and the pharmacokinetic parameters were calculated via WinNonlin.

## 3. RESULTS

### 3.1. *In vitro* inhibition activity, cytotoxicity and SARs of compounds 01–38

The *in vitro* inhibition activity of compounds 01–38 was systematically investigated against wild-type *P. falciparum* 3D7 and multi-drug-resistant *P. falciparum* Dd2. Dihydroartemisinin (DHA) was chosen as a positive control. The compounds' cytotoxicity in HepG2 and 293T cells was tested in parallel. The results are summarized in Table 1. Although the *in vitro* antimalarial activity of most of the compounds, compared with quisinostat, was poorer, the cytotoxicity was clearly lower, particularly for several compounds with favorable selectivity indexes greater than 1000. These results suggested that the narrow therapeutic window of quisinostat can be improved through structural modification. Herein, we concluded the following SARs of compounds 01–38: (I) replacing 4-aminomethylpiperidine with an 1-oxa-4,9-diazaspiro[5.5]undecane moiety slightly decreased the antimalarial activity but markedly decreased cytotoxicity

(quisinostat vs 01); (II) aliphatic and monocyclic aromatic and biphenyl CAP groups were not conducive to improved antimalarial activity (02–11 and 15 vs 01); (III) naphthyl, anthryl and other double-aromatic rings are tolerated in the CAP region, except 2-benzothiophenyl. (12–14 and 16–26 vs 01); (IV) treatment of azaindolyl group as CAP region or removal of *N*-methyl of 3-indolyl decreased the cytotoxicity and improved the selectivity index (27–33 vs 01); (V) introducing a substituent on the 3-indolyl group enhanced the potency against Dd2 and the selectivity index in HepG2 cells (34–38 vs 01). Thus, valuable SARs and structure-toxicity relationships were obtained through the systematic analysis of these 38 hydroxamic acid derivatives; among them, compounds 26, 33, 34 and 38 were the most potent compounds against 3D7 and Dd2, and exhibited better cellular safety than quisinostat; moreover, compound 30 showed moderate antimalarial activity but the best safety properties, with a selectivity index > 2316 in two cell lines.

### 3.2. *In vitro* metabolic stability of compounds 26, 30, 33, 34 and 38

Compounds 26, 30, 33, 34 and 38 were selected to investigate their stability in mouse liver microsomes *in vitro*. As shown in Table 2, all tested compounds were more stable than quisinostat. Among the compounds, the half-life ( $t_{1/2}$ ) of 30 was longest (> 150-fold longer than that of quisinostat and > 10-fold longer than that of compound 33). These results suggested that the structure of the CAP region strongly influences metabolic stability.

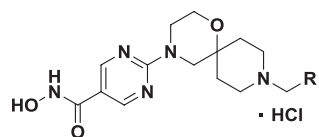
### 3.3. *In vitro* inhibition activity of compounds 30 and 33 against clinical multi-drug-resistant parasites

Compounds 30 and 33, two of the most stable compounds in mouse liver microsomes, were further evaluated for their antimalarial activity against clinical multi-drug-resistant lines (GB4, C2A, CP286 and 6218) via 72 h parasite-killing assays *in vitro*. Their  $IC_{50}$  values against the multi-drug-resistant lines (Table 3) were similar to those of the drug-sensitive line 3D7 (Table 1), thus implying that compounds 30 and 33 avoided cross resistance, possibly because of the differences in antimalarial mechanisms between these compounds and existing antimalarial drugs.

### 3.4. Compounds 30 and 33 upregulate histone acetylation in *P. falciparum* parasites

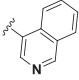
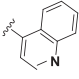
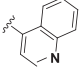
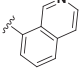
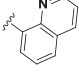
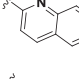
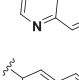
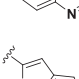
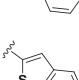
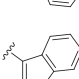
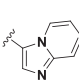
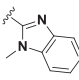
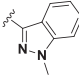
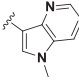
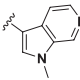

The mechanism of action of compounds 30 and 33 was explored by western blotting to detect the acetylation level of plasmodium histones (Figure 2). Plasmodium was pre-incubated with quisinostat and compounds 30 and 33 at 20-fold the  $IC_{50}$  (3D7) concentration for 4 h, and plasmodium protein was extracted to assess acetylation of H3. Compared with those in the DMSO control group,

## Research Article

**Table 1** | *In vitro* asexual erythrocyte-stage antimalarial activity and cytotoxicity of compounds **01–38**.

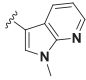
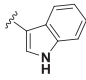
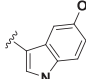
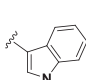
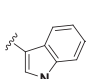
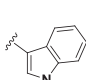
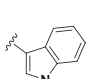
Compound	R	IC <sub>50</sub> (nM) <sup>a</sup> against <i>P. falciparum</i>		Cytotoxicity IC <sub>50</sub> (μM) <sup>a</sup>		Selectivity index <sup>b</sup> (3D7)	
		3D7	Dd2	HepG2	293T	HepG2	293T
Quisinostat <sup>c</sup>	-	5.21 ± 1.56	7.09 ± 0.01	0.04 ± 0.01	0.05 ± 0.01	8	9
01		10.51 ± 2.22	14.06 ± 0.11	3.66 ± 0.38	2.13 ± 0.20	349	203
02		107.73 ± 37.72	82.05 ± 4.50	13.85 ± 1.85	8.51 ± 0.46	129	79
03		144.60 ± 21.35	93.30 ± 4.60	> 20	> 20	> 138	> 138
04		62.63 ± 5.25	42.10 ± 5.80	14.33 ± 0.84	14.85 ± 0.61	229	237
05		17.24 ± 3.46	26.47 ± 0.06	4.32 ± 0.06	6.40 ± 2.33	250	371
06		36.13 ± 4.03	72.65 ± 0.28	12.24 ± 0.88	8.62 ± 3.10	339	239
07		56.86 ± 2.81	51.81 ± 1.83	6.25 ± 0.76	7.93 ± 1.30	110	140
08		45.35 ± 3.78	34.66 ± 4.11	9.22 ± 0.23	9.24 ± 1.15	203	204
09		73.99 ± 4.07	202.55 ± 19.87	16.32 ± 2.06	> 20	220	> 270
10		21.90 ± 2.79	29.89 ± 0.08	19.22 ± 1.57	16.17 ± 0.03	878	738
11		102.90 ± 2.40	54.33 ± 10.22	> 20	> 20	> 194	> 194
12		8.24 ± 0.67	7.95 ± 0.29	3.58 ± 0.38	3.65 ± 0.46	435	443
13		14.59 ± 2.04	8.83 ± 0.78	5.11 ± 0.11	4.59 ± 0.35	350	315
14		10.94 ± 2.73	9.19 ± 0.46	4.80 ± 0.04	5.83 ± 0.11	439	533
15		249.30 ± 0.99	88.95 ± 20.58	6.93 ± 0.23	7.83 ± 0.69	28	31

Table 1 | Continued

Compound	R	IC <sub>50</sub> (nM) <sup>a</sup> against <i>P. falciparum</i>		Cytotoxicity IC <sub>50</sub> (μM) <sup>a</sup>		Selectivity index <sup>b</sup> (3D7)	
		3D7	Dd2	HepG2	293T	HepG2	293T
16		10.33 ± 0.37	10.03 ± 0.20	3.13 ± 0.11	5.51 ± 1.77	303	533
17		7.55 ± 1.57	6.93 ± 0.22	3.85 ± 0.13	5.20 ± 0.22	510	688
18		7.28 ± 0.84	6.66 ± 0.58	4.79 ± 0.41	4.21 ± 1.11	657	578
19		7.40 ± 1.13	5.50 ± 0.11	2.12 ± 0.27	2.62 ± 0.50	287	354
20		14.63 ± 0.76	6.73 ± 0.32	2.96 ± 0.40	3.70 ± 0.89	202	253
21		13.28 ± 0.20	12.97 ± 2.04	4.03 ± 0.24	4.21 ± 0.54	303	317
22		14.55 ± 2.21	9.52 ± 0.52	6.22 ± 1.73	6.06 ± 0.93	427	416
23		18.37 ± 0.99	16.55 ± 1.85	8.50 ± 0.04	6.94 ± 1.61	463	378
24		12.14 ± 1.89	12.55 ± 0.48	8.06 ± 0.14	7.46 ± 1.44	664	615
25		46.44 ± 1.67	43.85 ± 0.45	4.09 ± 0.55	7.75 ± 0.20	88	167
26		6.25 ± 0.64	3.86 ± 0.84	2.12 ± 0.12	2.07 ± 0.21	340	331
27		19.39 ± 3.61	13.41 ± 2.14	7.34 ± 2.02	> 20	378	> 1031
28		9.67 ± 0.80	10.75 ± 0.29	3.54 ± 0.57	3.54 ± 0.43	366	366
29		7.50 ± 0.24	10.18 ± 0.39	7.93 ± 0.35	8.32 ± 0.73	819	859
30		8.64 ± 0.44	26.47 ± 0.06	> 20	> 20	> 2316	> 2316
31		16.58 ± 0.29	19.42 ± 2.92	> 20	12.53±0.792	> 1206	756

## Research Article

Table 1 | Continued

Compound	R	IC <sub>50</sub> (nM) <sup>a</sup> against <i>P. falciparum</i>		Cytotoxicity IC <sub>50</sub> (μM) <sup>a</sup>		Selectivity index <sup>b</sup> (3D7)	
		3D7	Dd2	HepG2	293T	HepG2	293T
32		14.81 ± 1.54	12.25 ± 0.55	8.03 ± 1.00	> 20	542	> 1350
33		5.72 ± 1.02	4.11 ± 0.02	> 20	9.12 ± 0.78	> 3494	1593
34		5.36 ± 0.41	3.96 ± 0.29	3.48 ± 0.40	1.26 ± 0.08	648	236
35		10.49 ± 0.43	6.27 ± 0.39	6.01 ± 1.00	3.48 ± 0.51	573	332
36		9.79 ± 1.28	4.97 ± 0.57	11.80 ± 1.09	4.07 ± 0.92	1205	416
37		8.80 ± 0.14	6.27 ± 0.59	3.93 ± 0.01	2.65 ± 0.41	446	301
38		6.49 ± 0.44	3.19 ± 0.09	6.90 ± 0.02	1.75 ± 0.16	1063	269
DHA <sup>c</sup>	-	2.68 ± 0.20	2.67 ± 0.02	nt	nt	nt	nt

<sup>a</sup>IC<sub>50</sub> values ± standard error of the mean; N = 2; 3D7: sensitive strain; Dd2: multi-drug resistant (MDR) strain; DHA: dihydroartemisinin. <sup>b</sup>Selectivity index (SI) = IC<sub>50</sub> (cytotoxicity)/IC<sub>50</sub> (3D7). Nt: not tested. <sup>c</sup>Data previously reported [27].

Table 2 | *In vitro* metabolic stability of compounds quisinostat, **26**, **30**, **33**, **34** and **38**

Compound	Metabolic stability in mouse liver microsomes	
	t <sub>1/2</sub> (min)	Cl <sub>int</sub> (mL/min/kg)
Quisinostat	13.31	410.10
26	23.60	231.26
30	2058.64	2.65
33	200.01	27.29
34	93.88	58.13
38	112.6	48.44

the acetylation levels of H3 in the drug-treated group, particularly the group treated with compound **30**, were all higher. Our results preliminarily demonstrated that the mechanism of action of these compounds involves inhibition of the PfHDAC enzyme, in agreement with results from our previous work.

### 3.5. *In vitro* inhibition activity of compounds **30** and **33** against human HDACs

In addition, we investigated the enzymatic inhibitory activity of compounds **30** and **33** against human HDACs. Among the tested enzymes, HDACs 1–3 and HDAC 8 are class I HDACs, HDAC 6 is a class II HDAC, and SIRT 2 is an NAD<sup>+</sup>-dependent class III HDAC [32]. As shown in Table 4, the activity of compounds **30** and **33** against class I/II HDACs was markedly lower than that of the lead compound quisinostat, thus potentially explaining the lower cytotoxicity of the derivatives in this work. Notably, for compound **30**, the IC<sub>50</sub> value against HDAC1 was nearly 60 times lower than that of quisinostat.

### 3.6. *In vivo* asexual erythrocyte-stage antimalarial activity of compound **30**

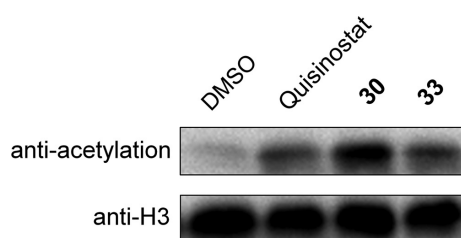
According to the *in vitro* experimental data, compound **30**, because of its low cytotoxicity and the best metabolic stability in liver microsomes, was selected as a candidate compound to evaluate its efficacy in a mouse model of *P. yoelii* infection (Figure 3). Herein, BALB/c mice were



**Table 3** | *In vitro* asexual erythrocyte-stage antimalarial activity of compounds **30** and **33** against clinical drug-resistant strains

Compound	IC <sub>50</sub> (nM) <sup>a</sup> against <i>P. falciparum</i>				
	GB4 <sup>b</sup>	C2A <sup>c</sup>	CP286 <sup>d</sup>	6218 <sup>e</sup>	6320 <sup>e</sup>
Quisinostat	1.7 ± 0.1	2.5 ± 0.1	2.0 ± 0.1	1.6 ± 0.0	1.9 ± 0.6
<b>30</b>	13.3 ± 1.6	15.9 ± 2.7	26.6 ± 0.3	14.4 ± 1.3	11.6 ± 1.0
<b>33</b>	10.9 ± 0.3	12.0 ± 1.1	9.3 ± 0.4	8.9 ± 1.3	7.8 ± 0.1
DHA	3.2 ± 1.2	3.7 ± 2.3	5.6 ± 2.3	5.9 ± 2.1	5.2 ± 3.7

<sup>a</sup>IC<sub>50</sub> values ± standard error of the mean; N = 2. <sup>b</sup>Drug resistance to chloroquine. <sup>c</sup>Drug resistance to quinine. <sup>d</sup>Drug resistance to sulfadoxine-pyrimethamine and mefloquine. <sup>e</sup>Drug resistance to artemisinin.

**Figure 2** | Acetylation of *P. falciparum* histones.**Table 4** | IC<sub>50</sub> of compounds **30** and **33** on human HDACs<sup>a</sup>

Compound	IC <sub>50</sub> (nM)					
	HDAC 1	HDAC 2	HDAC 3	HDAC 6	HDAC 8	SIRT 2
Quisinostat	< 0.5	1.1	2.1	34.9	9.2	>10000
<b>30</b>	27.4	38.9	103.7	132.5	216.2	>10000
<b>33</b>	10.2	15.1	45.2	66.0	150.8	>10000
Vorinostat	10.5	23.7	27.6	13.5	300.9	nt
Suramin	nt	nt	nt	nt	nt	5441

<sup>a</sup>Vorinostat and suramin were used as positive control drugs. Nt: not tested.

randomly divided into five groups, and the tested drugs were administered for 5 days after the day of inoculation with  $1 \times 10^5$  parasites. PPQ was chosen as a positive control and administered intraperitoneally, whereas quisinostat and compound **30** were administered orally. As shown in **Figure 3A**, all mice in the vehicle group died by day 7, thus indicating successful infection with *P. yoelii*. One mouse in the quisinostat-treated group died on day 6, presumably because of cumulative toxicity caused by continual administration, whereas compound **30** showed a good safety profile, and no mice died. We collected tail-vein blood from mice on day 6 (the first day after the end of drug administration), day 30 and day 60 and prepared blood smears to quantify parasitemia (**Figure 3B**). Although compound **30** did not completely kill the parasites on day 6, it resulted in

clearly lower parasitemia rates (3.13% in the 120 mg/kg group and 0.12% in the 150 mg/kg group) than that in the vehicle group (95.23%), with killing rates above 95%. Notably, no parasites were observed in mice on days 30 and 60, thus indicating that all surviving mice had been cured. Overall, compound **30** was shown to be safe and effective in this model.

### 3.7. *In vivo* pharmacokinetic study of compound **30**

The pharmacokinetic (PK) properties of compound **30** administered via intraperitoneal injection were further investigated in BALB/c mice (**Table 5**). The maximum concentration ( $C_{max}$ ) and area under the curve (AUC) of **30** were much higher than those of quisinostat. Higher plasma concentrations of the compound may result in more potent parasite killing *in vivo*. In addition, compound **30** displayed a slightly longer half-life ( $t_{1/2}$ ) than quisinostat, and it was the derivative with the longest  $t_{1/2}$  in the entire series.

## 4. DISCUSSION

In this work, we designed and synthesized a series of novel hydroxamic acid derivatives (**01–38**) based on the antitumor drug quisinostat as an antimalarial lead compound. The optimal compound, **30**, showed potent inhibitory activity against *P. falciparum* parasites (IC<sub>50</sub> =  $8.64 \pm 0.44$  nM against 3D7) and low cytotoxicity (IC<sub>50</sub> > 20  $\mu$ M against HepG2 and 293T). Further evaluation indicated that **30** exhibited strong killing efficacy against several multi-drug-resistant clinical *P. falciparum* strains and therefore may contribute to solving the treatment failures caused by drug resistance. Moreover, the *in vivo* efficacy of compound **30** indicated complete elimination of parasites in a mouse model of *P. yoelii* infection and showed a safety profile superior to that of the lead compound quisinostat. In addition, **30** exhibited good metabolic stability in liver microsomes and favorable PK properties in mice. Preliminary mechanistic research indicated that **30** killed *P. falciparum* parasites by inhibiting PfHDAC enzyme activity. Together, these results suggest that **30** is a prospective prototype drug for malaria therapy that warrants further optimization.

## Research Article

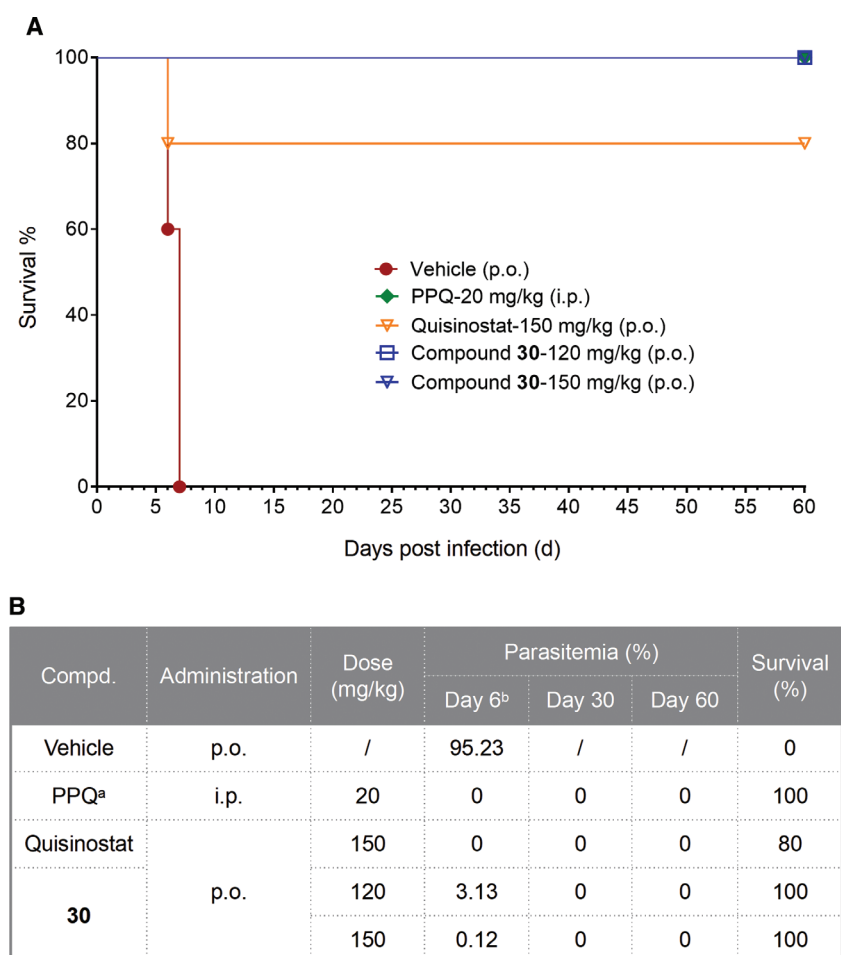


**Figure 3 | In vivo studies in a mouse model of *P. yoelii* infection.**

(A) Survival ratio. (B) Summary of activities of compounds against *P. yoelii* infection in mice. <sup>a</sup>PPQ, piperazine phosphate. <sup>b</sup>The day after the end of drug administration.

**Table 5 | PK parameters of compounds quisinostat and 30**

Parameter <sup>a</sup>	Quisinostat <sup>b</sup>	30
$C_{max}$ (ng/mL)	89	1112
$T_{max}$ (h)	0.08	0.25
$AUC_{last}$ (h $\times$ ng/mL)	157	1371
$AUC_{inf}$ (h $\times$ ng/mL)	180	1391
$t_{1/2}$ (h)	6.13	6.85
$CL_z/F$ (L/h/kg)	27.72	3.59
$V_z/F$ (L/kg)	245	35.53

<sup>a</sup>PK parameters in plasma after a single i.p. injection of 5 mg/kg compound in mice;  $C_{max}$ : maximum plasma or hepatic concentration;  $T_{max}$ : time to  $C_{max}$ ;  $AUC_{last}$ : area under the concentration–time curve from 0 to the last sampling time at which a quantifiable concentration was found;  $AUC_{inf}$ : area under the concentration–time curve from 0 to infinity;  $t_{1/2}$ : apparent elimination half-life;  $CL_z/F$ : apparent clearance;  $V_z/F$ : apparent volume of distribution. <sup>b</sup>Data previously reported [26].

#### ACKNOWLEDGEMENTS

We thank Dr. Didier Ménard for providing the artemisinin-resistant field isolates. This work was supported by the National Natural Science Foundation of China (82173689, 22037002, 81872747, 81903457 and 31972169), the National Key R&D Program of China (2017YFB0202600), the National Science and Technology Major Project (2018ZX10101004003001), the Key Collaborative Research Program of the Alliance of International Science Organizations (ANSO-CR-KP-2020-06), the Shanghai Frontiers Science Center of Optogenetic Techniques for Cell Metabolism (Shanghai Municipal Education Commission), the Innovative Research Team of High-level Local Universities in Shanghai, the Chinese Special Fund for State Key Laboratory of Bioreactor Engineering (2060204), the Pu'er Municipal Expert Workstation of L. J. and the Shanghai Sailing Program (19YF1412600).

#### CONFLICTS OF INTEREST

The authors declare that they have no known competing financial interests or personal relationships that could have appeared to influence the work reported in this paper.

## REFERENCES

- [1] *World malaria report 2021*. World Health Organization; 2021.
- [2] Hakizimana D, Ntuzimira C, Mbituyumuremyi A, Hakizimana E, Mahmoud H, Birindabagabo P, et al.: The Impact of Covid-19 on Malaria Services in Three High Endemic Districts in Rwanda: A Mixed-Method Study. *Malaria Journal* 2022, 21:48-64.
- [3] Teboh-Ewungkem MI, Ngwa GA: COVID-19 in Malaria-Endemic Regions: Potential Consequences for Malaria Intervention Coverage, Morbidity, and Mortality. *The Lancet Infectious Diseases* 2021, 21:5-6.
- [4] Duffy PE: Making a Good Malaria Vaccine Better. *Trends in Parasitology* 2022, 38:9-10.
- [5] Achan J, Mwesigwa J, Edwin CP, D'Alessandro U: Malaria Medicines to Address Drug Resistance and Support Malaria Elimination Efforts. *Expert Review of Clinical Pharmacology* 2018, 11:61-70.
- [6] Balikagala B, Fukuda N, Ikeda M, Katuro OT, Tachibana SI, Yamauchi M, et al.: Evidence of Artemisinin-Resistant Malaria in Africa. *New England Journal of Medicine* 2021, 385:1163-1171.
- [7] Uwimana A, Legrand E, Stokes BH, Ndikumana JM, Warsame M, Umulisa N, et al.: Emergence and Clonal Expansion of *in vitro* Artemisinin-Resistant *Plasmodium falciparum* kelch13 R561H Mutant Parasites in Rwanda. *Nature Medicine* 2020, 26:1602-1608.
- [8] Dondorp AM, Yeung S, White L, Nguon C, Day NP, Socheat D, et al.: Artemisinin Resistance: Current Status and Scenarios for Containment. *Nature Reviews Microbiology* 2010, 8:272-280.
- [9] Ashley EA, Phyo AP: Drugs in Development for Malaria. *Drugs* 2018, 78:861-879.
- [10] van der Pluijm RW, Amaratunga C, Dhorda M, Dondorp AM: Triple Artemisinin-Based Combination Therapies for Malaria - A New Paradigm? *Trends in Parasitology* 2021, 37:15-24.
- [11] Phillips MA, Lotharius J, Marsh K, White J, Dayan A, White KL, et al.: A Long-Duration Dihydroorotate Dehydrogenase Inhibitor (DSM265) for Prevention and Treatment of Malaria. *Science Translational Medicine* 2015, 7:296ra111.
- [12] Paquet T, Le Manach C, Cabrera DG, Younis Y, Henrich PP, Abraham TS, et al.: Antimalarial Efficacy of MMV390048, An Inhibitor of *Plasmodium* phosphatidylinositol 4-kinase. *Science Translational Medicine* 2017, 9:eaad9735.
- [13] Jimenez-Diaz MB, Ebert D, Salinas Y, Pradhan A, Lehane AM, Myrand-Lapierre ME, et al.: (+)-SJ733, A Clinical Candidate for Malaria that Acts Through ATP4 to Induce Rapid Host-Mediated Clearance of *Plasmodium*. *Proceedings of the National Academy of Sciences of the United States of America* 2014, 111:E5455-E5462.
- [14] Yang Y, Yu Y, Li X, Li J, Wu Y, Yu J, et al.: Target Elucidation by Cocrystal Structures of NADH-Ubiquinone Oxidoreductase of *Plasmodium falciparum* (PfNDH2) with Small Molecule to Eliminate Drug-Resistant Malaria. *Journal of Medicinal Chemistry* 2017, 60:1994-2005.
- [15] Zhan W, Visone J, Ouellette T, Harris JC, Wang R, Zhang H, et al.: Improvement of Asparagine Ethylenediamines as Anti-malarial *Plasmodium*-Selective Proteasome Inhibitors. *Journal of Medicinal Chemistry* 2019, 62:6137-6145.
- [16] Koehne E, Kreidenweiss A, Manego RZ, McCall M, Mombo-Ngoma G, Mackwitz MKW, et al.: Histone Deacetylase Inhibitors with High *in vitro* Activities Against *Plasmodium falciparum* Isolates Collected from Gabonese Children and Adults. *Scientific Reports* 2019, 9:17336.
- [17] Chua MJ, Arnold MSJ, Xu W, Lancelot J, Lamotte S, Spath GF, et al.: Effect of Clinically Approved HDAC Inhibitors on *Plasmodium*, *Leishmania* and *Schistosoma* Parasite Growth. *International Journal of Parasitology: Drugs and Drug Resistance* 2017, 7:42-50.
- [18] Hansen FK, Sumanadasa SDM, Stenzel K, Duffy S, Meister S, Marek L, et al.: Discovery of HDAC Inhibitors with Potent Activity Against Multiple Malaria Parasite Life Cycle Stages. *European Journal of Medicinal Chemistry* 2014, 82:204-213.
- [19] Beus M, Rajic Z, Maysinger D, Mlinaric Z, Antunovic M, Marijanovic I, et al.: SAHAQuines, Novel Hybrids Based on SAHA and Primaquine Motifs, as Potential Cytostatic and Antiplasmodial Agents. *ChemistryOpen* 2018, 7:624-638.
- [20] Diedrich D, Stenzel K, Hespings E, Antonova-Koch Y, Geburu T, Duffy S, et al.: One-pot, Multi-component Synthesis and Structure-Activity Relationships of Peptoid-Based Histone Deacetylase (HDAC) Inhibitors Targeting Malaria Parasites. *European Journal of Medicinal Chemistry* 2018, 158:801-813.
- [21] Mackwitz MKW, Hespings E, Eribe K, Scholer A, Antonova-Koch Y, Held J, et al.: Investigation of the *in vitro* and *in vivo* Efficacy of Peptoid-Based HDAC Inhibitors with Dual-Stage Antiplasmodial Activity. *European Journal of Medicinal Chemistry* 2021, 211:113065.
- [22] Huang Y, Dong G, Li H, Liu N, Zhang W, Sheng C: Discovery of Janus Kinase 2 (JAK2) and Histone Deacetylase (HDAC) Dual Inhibitors as a Novel Strategy for the Combinational Treatment of Leukemia and Invasive Fungal Infections. *Journal of Medicinal Chemistry* 2018, 61:6056-6074.
- [23] Andrews KT, Haque A, Jones MK: HDAC Inhibitors in Parasitic Diseases. *Immunology & Cell Biology* 2012, 90:66-77.
- [24] Chaal BK, Gupta AP, Wastuwidyaningtyas BD, Luah YH, Bozdech Z: Histone Deacetylases Play a Major Role in the Transcriptional Regulation of the *Plasmodium falciparum* Life Cycle. *PLoS Pathogens* 2010, 6:e1000737.
- [25] Mancio-Silva L, Lopez-Rubio JJ, Claes A, Scherf A: Sir2a Regulates rDNA Transcription and Multiplication Rate in the Human Malaria Parasite *Plasmodium falciparum*. *Nature Communications* 2013, 4:1530-1535.
- [26] Huang Z, Li R, Tang T, Ling D, Wang M, Xu D, et al.: A Novel Multistage Antiplasmodial Inhibitor Targeting *Plasmodium falciparum* Histone Deacetylase 1. *Cell Discovery* 2020, 6:93-107.
- [27] Li R, Ling D, Tang T, Huang Z, Wang M, Ding Y, et al.: Discovery of Novel *Plasmodium falciparum* HDAC1 Inhibitors with Dual-Stage Antimalarial Potency and Improved Safety Based on the Clinical Anticancer Drug Candidate Quisinosat. *Journal of Medicinal Chemistry* 2021, 64:2254-2271.
- [28] Li R, Ling D, Tang T, Huang Z, Wang M, Mao F, et al.: Repurposing of Antitumor Drug Candidate Quisinosat Lead to Novel Spirocyclic Antimalarial Agents. *Chinese Chemical Letters* 2021, 32:1660-1664.
- [29] Jiang L, Mu J, Zhang Q, Ni T, Srinivasan P, Rayavara K, et al.: PfSETvs Methylation of Histone H3K36 Represses Virulence Genes in *Plasmodium falciparum*. *Nature* 2013, 499:223-227.

## Research Article

- [30] Smilkstein M, Sriwilaijaroen N, Kelly JX, Wilairat P, Riscoe M: Simple and Inexpensive Fluorescence-Based Technique for High-throughput Antimalarial Drug Screening. *Antimicrobial Agents and Chemotherapy* 2004, 48:1803–1806.
- [31] Ishih A, Kawakami C, Todoroki A, Hirai H, Ohori K, Kobayashi F: Outcome of Primary Lethal and Nonlethal *Plasmodium yoelii* Malaria Infection in BALB/c and IFN-gamma Receptor-deficient Mice Following Chloroquine Treatment. *Parasitology Research* 2013, 112:773-780.
- [32] Varasi M, Thaler F, Abate A, Bigogno C, Boggio R, Carezzi G, et al.: Discovery, Synthesis, and Pharmacological Evaluation of Spiropiperidine Hydroxamic Acid Based Derivatives as Structurally Novel Histone Deacetylase (HDAC) Inhibitors. *Journal of Medicinal Chemistry* 2011, 54:3051-3064.